Results in Materials 21 (2024) 100517

Contents lists available at ScienceDirect

Results in Materials

journal homepage: www.sciencedirect.com/journal/results-in-materials

Effect of mixed alkali ions on the structural and spectroscopic properties of Nd^{3+} doped silicate glasses

Israel Montoya Matos [a,*], Naira M. Balzaretti [b,**]

[a] Universidad de Lima, Av. Javier Prado Este 4600, Lima, 15023, Peru
[b] Institute of Physics, Universidade Federal do Rio Grande do Sul, Porto Alegre (RS), 91501-970, Brazil

ARTICLE INFO

Keywords:
Vis-NIR spectroscopy
Luminescence
Judd-Ofelt theory
Nd^{3+}
Alkali silicates

ABSTRACT

In the present work the effect of alkali ions (Li, Na, K) and the combination of them on structural and spectroscopic properties of Nd^{3+} doped silicate glasses were systematically investigated. Results from infrared and Raman spectroscopy, as well as density and refractive index, were used to investigate the effect on the structural properties of the silicate glasses. Absorption and emission spectra of the glass samples were measured in the UV-VIS and NIR ranges. Relatively large, stimulated emission cross-section at 1.06 μm was obtained for samples containing a combination of alkali ions, especially with potassium. Moreover, the splitting induced by the Stark effect on the hypersensitive transition of Nd^{3+}, $^4I_{9/2} \rightarrow {}^4G_{5/2}$, $^2G_{7/2}$ was larger for the samples containing potassium, probably due to its larger ionic size. Judd-Ofelt theory was applied to evaluate the phenomenological intensity parameters Ω_2, Ω_4, Ω_6, transition probabilities, radiative lifetimes and branching ratios related to Nd^{3+} ions, calculated from optical absorption and luminescence spectra and the results were compared to the values obtained for different Nd-doped glasses reported in the literature.

1. Introduction

Trivalent rare-earth (RE) ions have a wide range of applications related to their sharp and intense electronic transitions in the visible and NIR regions, standing out their use as active media for laser and optical amplifiers [1–6]. From the scientific point of view, the energy, profile and intensity of the absorption and emission bands depend on the distribution of charges in the first coordination shell of RE ions and, therefore, their optical spectra can be used as structural probes for estimating local field parameters within a given host glass [7]. Ratnakaram et al. [8–12], studied the optical properties of Nd^{3+} ions in mixed alkali borate, fluoroborate and chloroborate glasses. De La Rosa-Cruz et al. [13] investigated the spectroscopic characterization of Nd^{3+} ions in barium fluorophosphates glasses.

Silica may be an ideal host matrix for Nd^{3+} ions for using as amplifier for long distance optical communications due to its high thermal stability, transparency from UV to NIR, low thermal expansion coefficient and low refractive index [14,15]. However, a fully polymerized silica glass would not have non-bridging oxygen atoms required to fulfill the charge balance of the RE ions, resulting in low solubility of high-field strength RE ions. In fact, clustering and microscale phase separation have been observed even for very small amounts of RE ions on silicate glasses [16]. This segregation may induce fluorescence quenching due to the non-radiative energy transfer between the RE ions within each cluster, decreasing the amplification efficiency of the glass fibers. However, results obtained from EXAFS analysis showed that the addition of Al, P or alkali ions in silica was able to open the silicate network, creating non-bridging oxygen atoms that allow a homogeneous dispersion of RE ions, avoiding segregation [16].

In the present work the spectroscopic properties of Nd^{3+} ions were used to investigate the local structure of alkali (Li, Na, K) and mixed alkali (LiNa, NaK, KLi) oxides in silica. It is known for a long time that the gradual replacement of one alkali oxide by another induces nonlinear changes in certain physical properties of glasses [17,18] and the explanation for this effect in terms of the atomic structure is not simple due to the amorphous nature of the glass. In 1987, LaCourse [19] proposed a model for the effect of the mixed alkali oxides considering that during cooling, the alkali ions tend to form their own environment of "balance" surrounded by non-bridged oxygen atoms. This effect depends on the difference between the radii of the two ions as well as on

* Corresponding author.
** Corresponding author.
E-mail addresses: imontoya@ulima.edu.pe (I. Montoya Matos), naira@if.ufrgs.br (N.M. Balzaretti).

https://doi.org/10.1016/j.rinma.2023.100517
Received 10 October 2023; Received in revised form 11 December 2023; Accepted 21 December 2023
Available online 25 December 2023
2590-048X/© 2023 The Authors. Published by Elsevier B.V. This is an open access article under the CC BY-NC-ND license (http://creativecommons.org/licenses/by-nc-nd/4.0/).

Table 1
Chemical composition of the glass samples.

Sample notation	Glass compositions (mol%)
LS-Nd	33.0 Li_2O + 66.0 SiO_2 + 1.0 Nd_2O_3
NS-Nd	33.0 Na_2O + 66.0 SiO_2 + 1.0 Nd_2O_3
KS-Nd	33.0K_2O + 66.0 SiO_2 + 1.0 Nd_2O_3
LNS-Nd	16.5 Li_2O + 16.5 Na_2O + 66.0 SiO_2 + 1.0 Nd_2O_3
NKS-Nd	16.5 Na_2O + 16.5 K_2O + 66.0 SiO_2 + 1.0 Nd_2O_3
LKS-Nd	16.5 Li_2O + 16.5 K_2O + 66.0 SiO_2 + 1.0 Nd_2O_3

their electronic polarizabilities.

2. Materials and methods

2.1. Sample preparation

Analytical reactants Li_2CO_3, Na_2CO_3, K_2CO_3, SiO_2 and Nd_2O_3 (99.99 % purity grade from Sigma-Aldrich) and melt quenching technique were used for sample preparation. Table 1 shows the glass compositions investigated in this work.

Since carbonates and silica are highly hygroscopic, they were initially dried at 200 °C during 1–2 h. The reactants were, then, mixed in a high-energy planetary mill for 2 h at 150 rpm. The mixture was placed in a platinum crucible, heated at 700–800 °C to eliminate CO_2 [20] and then, melted at 1550 °C for 2h in air. The melted was quickly poured into a preheated stainless-steel mold and annealed at 350 °C for 4h. After that, it was cooled down slowly to room temperature.

2.2. Analytical techniques

Density of the samples was measured using the Archimedes method (analytical balance Shimadzu AUW220D 0.1mg/0.01 mg) with distilled water as the immersion liquid. The refractive index was measured using a SOPRA GES-5E ellipsometer. The amorphous nature of the sample was confirmed by X-ray powder diffraction using a diffractometer Siemens model D500. The FTIR transmittance spectra were measured using a Bomem MB100 spectrometer using KBr pellets. Raman spectra were measured using HeNe laser as excitation source. The absorption spectrum of the polished glasses was measured using a Shimadzu UV-2450 UV–Vis spectrometer in the 300–1000 nm range and the results were used to calculate the absorption cross section using the Beer- Lambert law. Photoluminescence (PL) data were measured using CryLas GmbH 488 nm CW laser as pumping source. The PL signal was dispersed by an Acton SP2300 monochromator and detected by a Pixis 256E CCD. The detected signal was feed to a SR430 multichannel analyzer and transferred to a computer running acquisition software.

2.3. Optical properties

The intensity of the absorption bands of RE ions in a host glass can be expressed as oscillator strengths, successfully estimated by the Judd-Ofelt (JO) theory [21,22] which defines a set of three parameters (Ω_2, Ω_4, Ω_6) susceptible to the environment of the RE ion. The parameter Ω_2 is related to the covalence of the metal ligand bond while Ω_4 and Ω_6 is related to the rigidity of the host matrix. The radiative transition probabilities, radiative lifetime and branching ratios can be calculated from the JO parameters. Glass composition has influence on the stimulated cross section, bandwidth and refractive index and, therefore, on the JO parameters. Due to the characteristic lack of long-range order in glasses, the local environment of the RE ions should be slightly different from one site to another, resulting in broad absorption bands. The crystal-field splitting is also responsible for broadening of these bands [7].

It has been assumed that in oxide glasses, the RE ion has 8 neighboring oxygen atoms shared with the corners of the glass forming

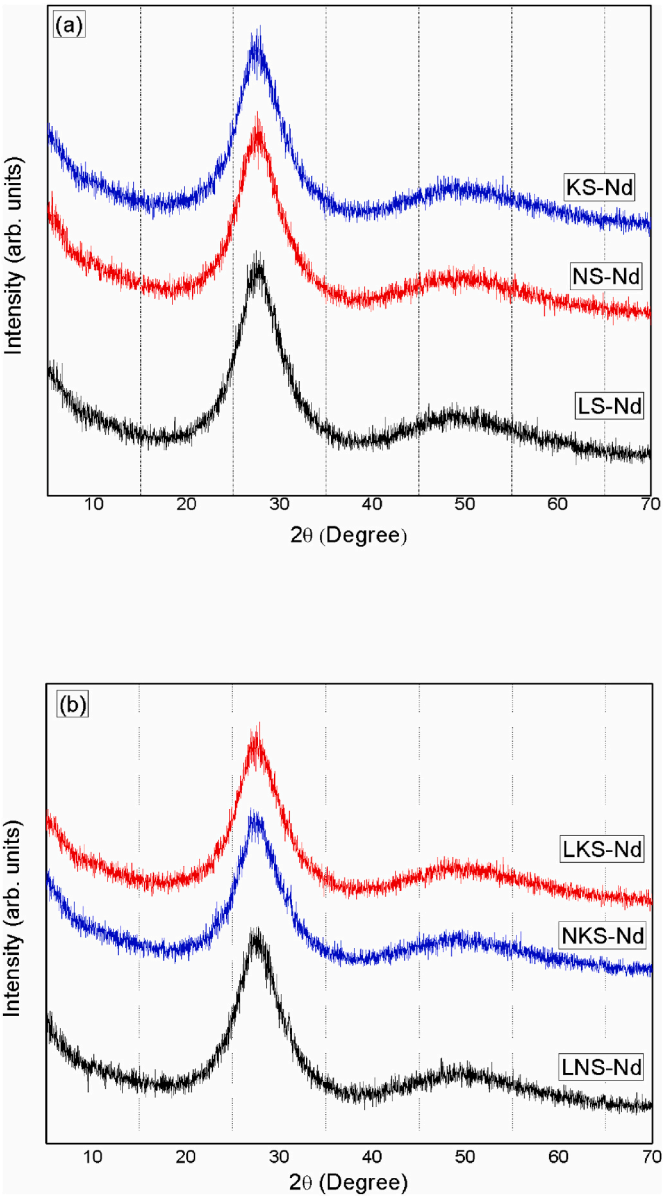

Fig. 1. X-ray diffraction pattern, (a) alkali silicate glasses, (b) alkali mixed silicate glasses.

tetrahedra. In the case of Nd^{3+}, its $4f^3$ electrons are shielded by the $5s^25p^6$ electrons, being weakly perturbed by the surrounding atoms. Changes in the energies of the $^{2S+1}L_J$ multiplets of Nd^{3+} when it is embedded in a glass host arise from its charge transfer with the ligand, called nephelauxetic effect, which induces a contraction of the energy level structure of the ion in the glass [7]. For lanthanide ions there are certain f-f transitions which are exceptionally sensitive to the local environment, known as hypersensitive transitions ($\Delta J \leq 2$, $\Delta L \leq 2$ and $\Delta S = 0$). For Nd^{3+}, they correspond to the $^4I_{9/2} \rightarrow {}^4G_{5/2}$ and $^2G_{7/2}$ transitions, which are in the visible range. The addition of alkali ions as network modifiers in oxide glasses induces the formation of non-bridging oxygen atoms, changing the forming cation coordination number. This effect induces changes in the lanthanide-oxygen distances and, therefore, should affect the optical properties of the RE ion [7].

3. Results and discussions

The X-ray diffraction pattern of the samples glass shown in Fig. 1 confirmed its amorphous structure.

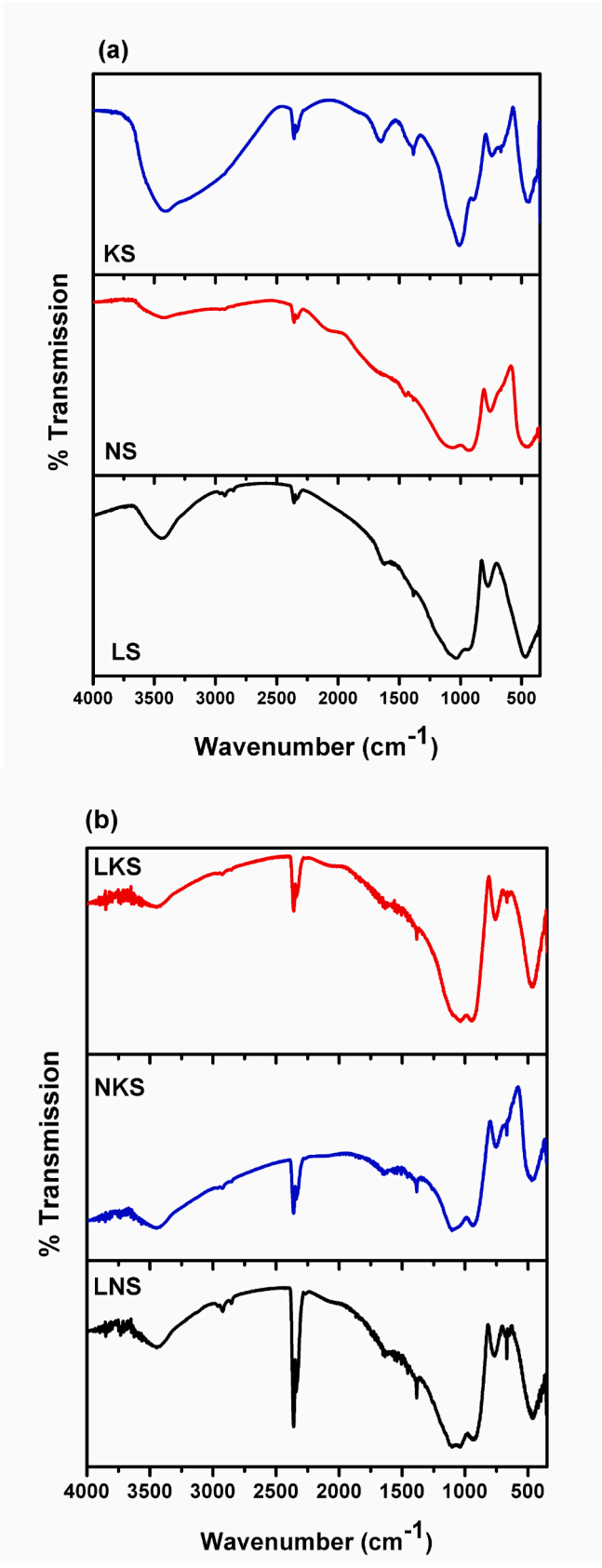

Fig. 2. FTIR spectra of the alkali (a) and mixed alkali (b) silicate glasses. (the narrow band close to 2300 cm-1 is due to CO_2 from the ambient).

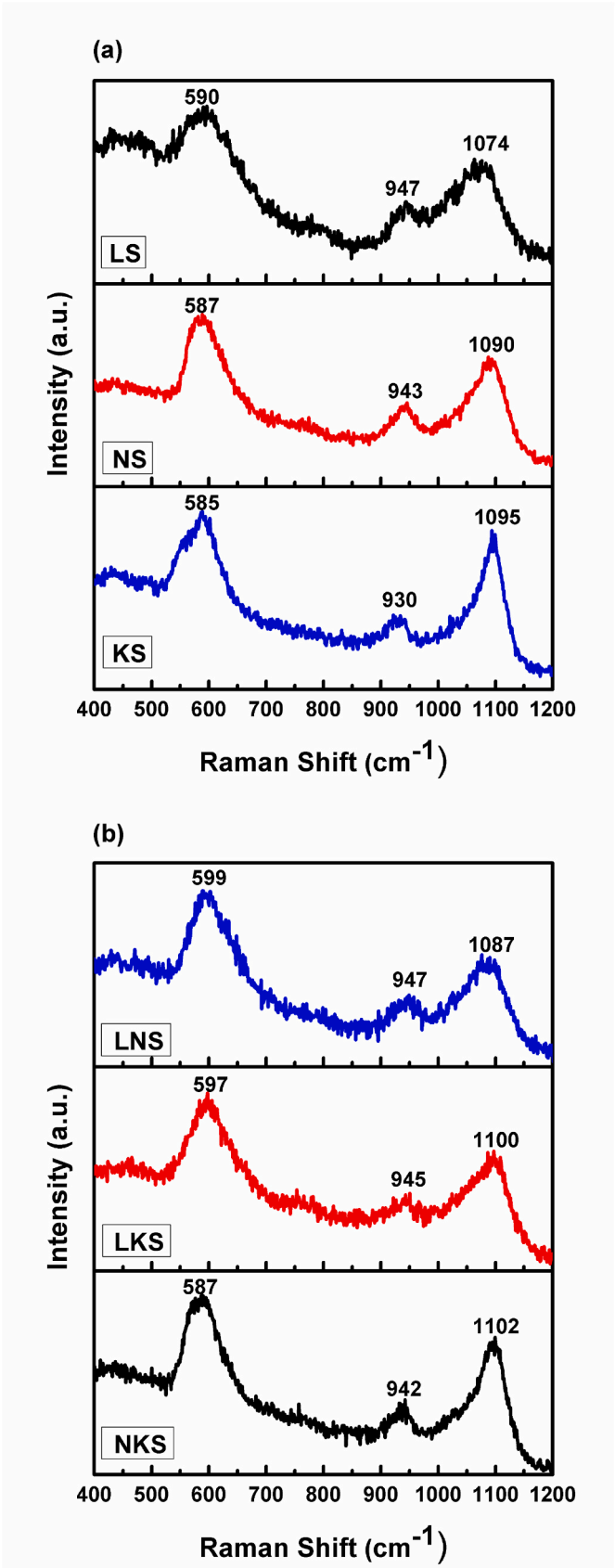

Fig. 3. Raman spectra of the alkali (a) and mixed alkali (b) metal silicate glasses doped with Nd^{3+}.

Table 2
Physical properties of Nd^{+3} doped alkali and mixed alkali metal ion silicate samples.

Sample	LS-Nd	NS-Nd	KS-Nd	LNS-Nd	NKS-Nd	LKS-Nd
Density, ρ (gm/cm^3) (±0.0005)	2.4951	2.4809	2.4694	2.4704	2.4935	2.5556
Refractive index (n) (585 nm)	1.6110	1.5860	1.4450	1.4880	1.4320	1.4810
Concentration of Nd^{3+}, N (x10^{20} ions/cm^3)	2.23	1.92	1.68	2.05	1.80	1.97
Molar Volume (V_m) (cm^3/mol)	27.0135	31.4376	35.8893	29.4275	33.4106	30.5265
Polaron radius, r_p (Å)	6.6447	6.9893	7.3048	6.8370	7.1326	6.9211
Interionic distance, r_i (nm)	1.6492	1.7347	1.8130	1.6970	1.7703	1.7178
Field strength, F (x10^{16}cm^{-2})	6.7946	6.1412	5.6222	6.4178	5.8970	6.2628
Reflection losses (R_L) (x10^{-2})	5.4760	5.1349	3.3125	3.8471	3.1552	3.7586
Molar refraction (R_m) (cm^3/mol)	9.3780	10.5506	9.5519	8.4784	8.6658	8.6873
Optical dielectric constant	1.5953	1.5153	1.0880	1.2141	1.0506	1.1933
Dielectric constant (ε)	2.5953	2.5153	2.0880	2.2141	2.0506	1.1933
Molar polarizability (α_m) x 10^{-22}cm^3	3.7279	4.1828	3.7868	3.3612	3.4355	3.4440

Fig. 2 shows the FTIR spectra of the alkali and mixed alkali silicate glasses. Amorphous silica can be considered as a random network of Si–O tetrahedra whose infrared vibrations would be at ~1100 cm^{-1} and between 400 and 600 cm^{-1}. The band at ~1100 cm^{-1} is due to the Si–O stretching within the tetrahedra and the band at ~950 cm^{-1} is due to the stretching of the non-bridged terminal Si–O. The band at ~790 cm^{-1} is due to the stretching of the bridged Si–*O*–Si between tetrahedra and the band at ~460 cm^{-1} is due to bending modes involving Si–*O*–Si and O–Si–O. According to Muralidharan et al. [23] the Si–O–Si and Si–OH bending modes are sharpened with the introduction of Nd^{3+} ion since the introduction of rare earth ions alters the environment of the defect centers in silica. Also, the addition of alkali ions would decrease the local symmetry due to the formation of non-bridging oxygen bonds, giving rise to a stretching mode at ~950 cm^{-1} [24]. The band close to ~3500 cm^{-1} is related to OH group. Comparing the spectra shown in Fig. 2a, all of them present a shoulder at ~950 cm^{-1}, more pronounced for LS and NS samples, indicating the formation of non-bridged terminal Si–O. Also, the relative intensities of the peaks corresponding to the Si–O stretching from the tetrahedra and from the non-bridged Si–O are practically the same for LS and NS samples, but, for KS sample, the band at ~1100 cm^{-1} is narrower, suggesting that K is not so effective in creating non-bridged oxygen atoms in silica as Li and Na alkali ions. The intensity of the band related to OH group is also more pronounced for KS sample, which is highly hygroscopic. Fig. 2b shows the spectra for the mixed alkali samples which are very similar in all the spectral range investigated, even for samples containing K.

Fig. 3 shows the Raman spectra of the samples. For pure silica, the Raman spectrum contains a large and asymmetric band at ~440 cm^{-1} related to bonded oxygen and silicon from the glassy network and a sharp band at ~492 cm^{-1} related to the SiO_4 tetrahedra. A broad band at ~800 cm^{-1} is related to the network of the SiO_2 glass, a band at ~600 cm^{-1} is related to defects, bands at 1060 and 1190 cm^{-1} are related to Si–*O*–Si vibrations and a band at ~950 cm^{-1} is related to chains of SiO_4 tetrahedra [25]. According to Matson et al. [24], the introduction of alkali ions in the silica network induces changes in the Raman spectrum depending on the ion type and concentration. The stretching of non-bonding oxygen on SiO_4 tetrahedra due to the alkali ion appears at ~1100 cm^{-1}. If the band at ~440 cm^{-1}, related to the silica network, remains in the alkali silicate glass, it indicates that the distribution of the ions is not homogeneous. The intensity of this band would be related to the trend of ion cluster formation, detected for the smaller ions, Li and Na, but not for the larger ones, K, Rb and Cs, that would be randomly distributed in the silica glass surrounded by non-bonding oxygen atoms [24,25]. Fig. 3a shows that, in fact, a large band at ~440 cm^{-1} still exists for the LS sample, suggesting formation of Li clusters, but it was not clearly observed for the other samples, indicating homogeneous distribution of the alkali ions in the silica glass except for LS sample. An intense band is observed for all samples close to 600 cm^{-1}, related to defects in the silica network, probably induced by the alkali ions (creation of non-bonding oxygen atoms). Consistently, the bands close to

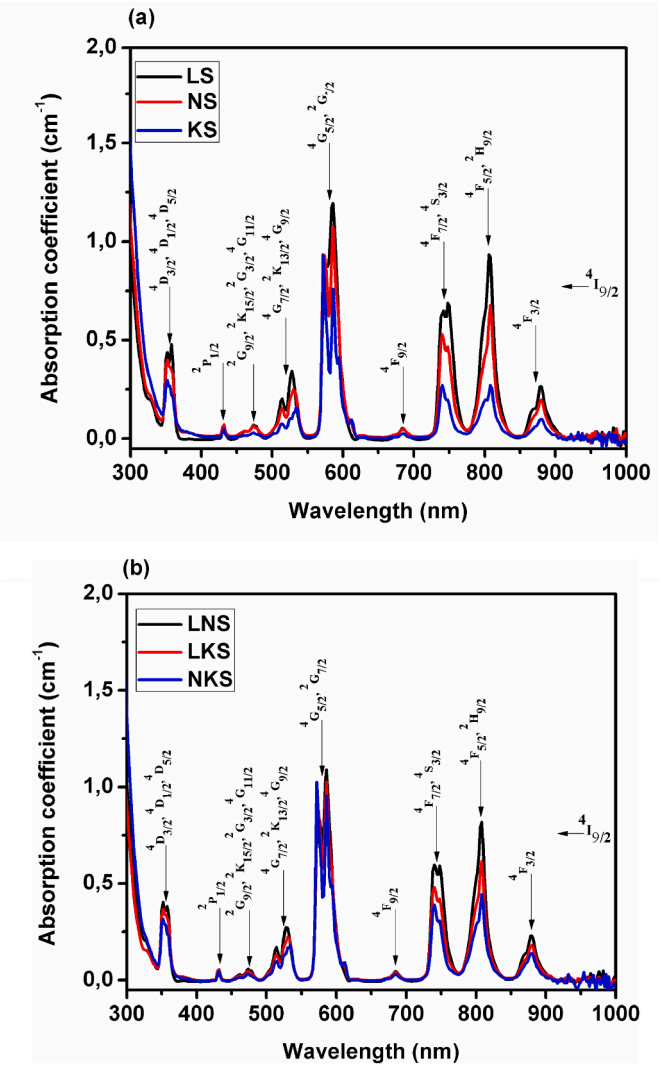

Fig. 4. Room temperature optical absorption spectra of the alkali (a) and mixed alkali (b) metal silicate glasses doped with Nd^{3+}.

~1100 cm^{-1} and ~950 cm^{-1} are also observed for all samples while the band at ~800 cm^{-1}, related to the silica network, was not observed. The Raman spectra of mixed alkali glasses are shown in Fig. 3b, where the low intensity of the band around 440 cm^{-1} indicate little formation of alkali clusters. The most intense band occurs around 600 cm^{-1} with small shifts to the right due to the creation of non-binding oxygen due to the presence of the alkali ion mixture.

Table 3
Nephelauxetic parameters, β, and bonding parameter, δ, calculated from the average value of β. The last column presents the wavenumbers corresponding to the absorption bands of the free Nd^{3+} ions.

Transition from $^4I_{9/2}$ →	LS-Nd	NS-Nd	KS-Nd	LNS-Nd	NKS-Nd	LKS-Nd	ν cm^{-1} [28]
$^4F_{3/2}$	0.993805	0.991536	0.990401	0.993805	0.991536	0.99267	11460
$^4F_{5/2}$, $^2H_{9/2}$	0.990985	0.988512	0.986039	0.988512	0.986039	0.987316	12535
$^4F_{7/2}$, $^4S_{3/2}$	0.99963	1.002296	1.003704	0.990222	0.992889	0.991556	13500
$^4F_{9/2}$	0.99449	0.993061	0.991633	0.995986	0.993061	0.99449	14700
$^4G_{5/2}$, $^2G_{7/2}$	0.985213	0.983544	0.981818	0.983544	0.980322	0.981818	17380
$^2K_{13/2}$, $^4G_{7/2}$, $^4G_{9/2}$	0.978507	0.976647	0.96931	0.978507	0.96931	0.974787	19355
$^2K_{15/2}$, $^2G^2_{9/2}D_{3/2}$, $^4G_{11/2}$	0.996042	0.993969	0.991849	0.996042	0.991849	0.993969	21225
$^2P_{1/2}$	0.997892	0.995613	0.99329	0.997892	0.995613	0.997892	23250
$^4D_{3/2}$, $^4D_{1/2}$, $^4D_{5/2}$	0.981121	0.975657	0.972925	0.995061	0.992224	0.997898	28550
$\overline{\beta}$	0.990854	0.988982	0.986774	0.991064	0.988094	0.990266	
Δ	0.9231	1.1141	1.3403	0.9017	1.205	0.9829	

Table 4
Experimental and calculated oscillator strengths (x10^{-6}) of Nd^{3+} in alkali and mixed alkali silicate glasses.

Transitions from 4I9/2 →	LS-Nd		NS-Nd		KS-Nd		LNS-Nd		NKS-Nd		LKS-Nd	
	f_{exp}	f_{cal}	f_{exp}	f_{cal}	f_{exp}	f_{cal}	f_{exp}	f_{cal}	f_{exp}	f_{cal}	f_{exp}	f_{cal}
$^4F_{3/2}$	1.47	1.67	1.16	1.49	0.84	1.18	1.38	1.69	1.39	2.54	1.01	1.42
$^4F_{5/2}$, $^2H_{9/2}$	5.27	5.20	4.05	4.16	2.69	2.91	4.91	5.12	5.37	5.71	3.70	3.83
$^4F_{7/2}$, $^4S_{3/2}$	5.01	5.30	3.92	4.03	2.60	2.54	4.94	5.20	4.96	4.75	3.56	3.62
$^4F_{9/2}$	0.36	0.42	0.29	0.33	0.13	0.22	0.33	0.41	0.32	0.42	0.26	0.29
$^4G_{5/2}$, $^2G_{7/2}$	14.2	14.3	15.0	15.1	17.3	17.3	15.0	15.2	23.2	23.3	14.2	14.2
$^2K_{13/2}$, $^4G_{7/2}$, $^4G_{9/2}$	4.50	3.51	3.99	3.15	3.22	2.71	4.46	3.56	5.13	4.69	3.63	2.95
$^2K_{15/2}$, $^2G^2_{9/2}D_{3/2}$, $^4G_{11/2}$	1.13	0.92	0.89	0.78	0.61	0.58	0.93	0.92	0.90	1.18	0.79	0.72
$^2P_{1/2}$	0.38	0.43	0.37	0.40	0.33	0.32	0.39	0.44	0.37	0.73	0.31	0.38
$^4D_{3/2}$, $^4D_{1/2}$, $^4D_{5/2}$	7.81	7.94	7.36	7.40	6.03	6.00	8.18	8.23	13.4	13.1	7.09	7.10
Γ^2_{rms} x 10^{-7}	4.44		3.79		2.70		4.22		5.75		3.32	

Table 2 shows some physical properties of the samples, calculated from the experimental results for density (ρ) and refractive index. The density values are like the results found in the literature for alkali silicates [25]. These properties, including the concentration of Nd^{3+} ions, depend on the specific alkali ion, as should be expected. The value of the Nd^{3+} ion concentration decreases as the size of the alkali ion increases and, for the mixed alkali silicates, it is in-between the values for the individual alkali silicates. The larger the volume of the alkali ion, the lower the values of the field strength, refractive index and density. Consistently, the polaron radius and interionic distance, on the other hand, are larger for the larger alkali ions.

Fig. 4 shows the optical absorption spectra measured for Nd^{3+} doped alkali and mixed alkali silicate samples, containing the identification of the correspondent electronic transitions from the ground state $^4I_{9/2}$. It is possible to see that the relative intensities of the absorption bands are different for each sample due to the distinct local fields surrounding the Nd^{3+} ions in these host glasses. Considering the hypersensitive transition of Nd^{3+}, $^4I_{9/2} \rightarrow {}^4G_{5/2}$, $^2G_{7/2}$, the splitting induced by the Stark effect is clearly seen, been more pronounced for the samples containing K, which has the larger ionic radius of the alkali ions investigated in this work. The relative intensities of the Nd^{3+} bands and the extent to which the fine structure of these bands can be observed is related to the Nd–O interaction and polarization of oxygen ions in the presence of the network former ions. For alkali modifiers with the same charge, the smallest ion, Li^+, should introduce the largest polarization and lead to the strongest ligand field. Conversely, the weakest ligand field should be for the largest ion, K^+. According to Giri et al. [26], glassy alkali silicates containing Li and Na tend to be covalently packed while K tends to induce ionic packing due to its larger volume and coordination number. According to the results for polaron ratios and field strengths presented in Table 2, the same correlation was observed for the mixed alkali silicates.

The nephelauxetic parameter, β, of an absorption transition is related to the covalence between the RE ion and the surrounding ligands and it is given by $\beta = \upsilon/\upsilon_f$, where u_f and u are the wavenumbers of the absorption bands of the free ion (in solution) and the probe ion in a given host matrix, respectively [27]. The bonding parameter is given by $\delta = [(1 - \overline{\beta}))/\overline{\beta}] * 100$, where $\overline{\beta}$ is the average nephelauxetic parameter considering all the absorption bands. Table 3 shows the values for these parameters calculated for the alkali and mixed alkali silicates. The wavenumbers corresponding to the free Nd^{3+} ion is shown in the last column [28]. The value of δ may be positive or negative, depending on the interaction between the RE ion and the ligands, indicating covalent or ionic bonding, respectively [28–30]. The positive values shown in Table 4 indicate a covalent interaction between Nd^{3+} and the ligand ion in the alkali silicates investigated. This was not the case observed by Kumar et al. [31] for Nd^{3+} ion in alkali lead zinc borate glasses, where the bonding parameter had negative values.

The oscillator strengths of the absorption transitions were calculated using the JO theory [21,22] to determine the parameters Ω_λ ($\lambda = 2$, 4 and 6) following the least squares fitting approximation method. The results are shown in Tables 4 and 5. The relatively small rms deviations between experimental and calculated spectral intensities demonstrate the validity of the JO theory for these samples. The spectral intensities are smaller for the alkali and mixed alkali silicates containing potassium compared to lithium and sodium. The opposite effect was observed for alkali and mixed alkali lead zinc borate glasses doped with Nd^{3+} [32].

Table 5 shows the Judd-Ofelt intensity parameters Ω_λ ($\lambda = 2$, 4 and 6) for the alkali and mixed alkali silicate samples investigated in this work, compared to the values found in the literature for different glass hosts. The spectroscopic quality factor $X = \Omega_4/\Omega_6$ is used to predict the stimulated emission in a laser active medium [32,36,37].

Considering Li and Na, the value of Ω_2 is very similar for silicate, phosphate and lead zinc borate glasses and it is larger for borate glass, suggesting that the RE site shows higher asymmetry for this glass composition. Glasses containing K show larger values of Ω_2 for silicate

Table 5
Judd Ofelt parameters (x 10^{-20} cm^2) and spectroscopic quality factor for Nd^{3+} doped alkali and mixed alkali metal silicate glasses compared to the values found in the literature.

Glass composition	Ω_2	Ω_4	Ω_6	c = Ω_4/Ω_6
LS (33.0 Li_2O + 66.0 SiO_2 + 1.0 Nd_2O_3) this work	3.71	3.68	4.14	0.88
30 Li_2O+70B_2O_3 [33]	4.20	3.89	4.74	0.82
30 Li_2O+60P_2O_5+10Al_2O_3 [33]	3.71	4.70	5.15	0.91
20 Li_2O + 53 B_2O_3 + 15 PbO + 10 ZnO + 2 Nd_2O_3 [31]	3.51	4.61	4.83	0.95
NS (33.0 Na_2O + 66.0 SiO_2 + 1.0 Nd_2O_3) this work	3.84	3.06	2.72	1.11
30 Na_2O+70B_2O_3 [33]	4.91	3.28	4.51	0.72
30 Na_2O+60P_2O_5+10Al_2O_3 [33]	3.82	4.74	5.53	0.86
20 Na_2O + 53 B_2O_3 + 15 PbO + 10 ZnO + 2 Nd_2O_3 [31]	3.84	4.59	4.99	0.92
KS (33.0K_2O + 66.0 SiO_2 + 1.0 Nd_2O_3) this work	5.46	2.81	1.85	1.51
30 K_2O+70B_2O_3 [33]	4.94	3.10	3.42	0.91
30 K_2O+60P_2O_5+10Al_2O_3 [33]	3.94	4.79	5.61	0.85
20 K_2O + 53 B_2O_3 + 15 PbO + 10 ZnO + 2 Nd_2O_3 [31]	6.07	3.88	5.68	0.68
LNS (16.5 Li_2O + 16.5 Na_2O + 66.0 SiO_2 + 1.0 Nd_2O_3) this work	3.84	3.62	3.82	0.95
16 Li_2O+16 Na_2O+67B_2O_3 [9]	8.39	6.51	10.01	0.65
10 Li_2O + 10 Na_2O + 53 B_2O_3 + 15 PbO + 10 ZnO + 2 Nd_2O_3 [31]	3.63	5.15	5.19	0.99
NKS (16.5 Na_2O + 16.5 K_2O + 66.0 SiO_2 + 1.0 Nd_2O_3) this work	5.89	6.29	3.45	1.82
15 Na_2O+15 K_2O+70B_2O_3 [34]	10.73	7.31	7.47	0.98
15 Na_2O+15 K_2O+69P_2O_5 [35]	6.94	6.85	9.61	0.71
10 Na_2O + 10 K_2O + 53 B_2O_3 + 15 PbO + 10 ZnO + 2 Nd_2O_3 [31]	4.49	5.64	5.62	1
LKS (16.5 K_2O + 16.5 Li_2O + 66.0 SiO_2 + 1.0 Nd_2O_3) this work	3.88	3.21	2.63	1.22
10 Li_2O + 10 K_2O + 53 B_2O_3 + 15 PbO + 10 ZnO + 2 Nd_2O_3 [31]	3.89	5.41	5.52	0.98

and lead zinc borate glasses. As can be seen, the larger the alkali ion, the larger is the Ω_2 value, independent of the glass composition. For the mixed alkali glasses, large values of Ω_2 have been obtained for borate glasses containing Li and Na, and Na and K. The values obtained in this work are similar to the values obtained for lead zinc borate glasses. Very low values of Ω_4 and Ω_6 were obtained for KS sample, suggesting lower rigidity compared to the other compositions investigated and to other glass hosts. The values of Ω_6 for alkali silicates are consistently lower than the values for borates, phosphates and lead zinc borate glasses. The values for the spectroscopic quality factor are larger than 1 for NS, KS, NKS and LKS samples, while the values found in the literature for borate, phosphate and lead zinc borate glasses containing alkali ions are smaller than 1, as shown in Table 5.

The luminescence spectra of the samples in the NIR region, obtained under excitation at 488 nm, are shown in Fig. 5, containing the characteristic Nd^{3+} bands at 890 nm, 1054 nm and 1330 nm, assigned to the transitions $^4F_{3/2} \rightarrow {}^4I_{9/2}$, $^4F_{3/2} \rightarrow {}^4I_{11/2}$ and $^4F_{3/2} \rightarrow {}^4I_{13/2}$, respectively. The intensity of the $^4F_{3/2} \rightarrow {}^4I_{11/2}$ laser transition is dependent on the so-called spectroscopic quality parameter, $c = \Omega_4/\Omega_6$ [35,38,39]. The χ values found in this work is in-between 0.88–1.82, which are well within the range of 0.51–1.40 found in Nd^{3+}-doped crystals. In this range both $^4F_{3/2} \rightarrow {}^4I_{9/2}$ and $^4F_{3/2} \rightarrow {}^4I_{11/2}$ laser channels possess equal probability for laser action [40–42]. The splitting of these bands, related to the Stark effect, and the peak intensities are more pronounced in the presence of K, compared to Li and Na. The same behavior was observed for the mixed alkali silicates, where the presence of K increases the splitting and the intensity of the luminescence bands. The size of the alkali ion (or the combination of them) affects the ligand field at the RE site and, therefore, the transition probabilities. The JO intensity parameters were used to calculate the radiative transition probabilities (A_{rad}), branching ratios (β_R) and radiative lifetimes (τ_R), shown in Table 6. The radiative lifetime

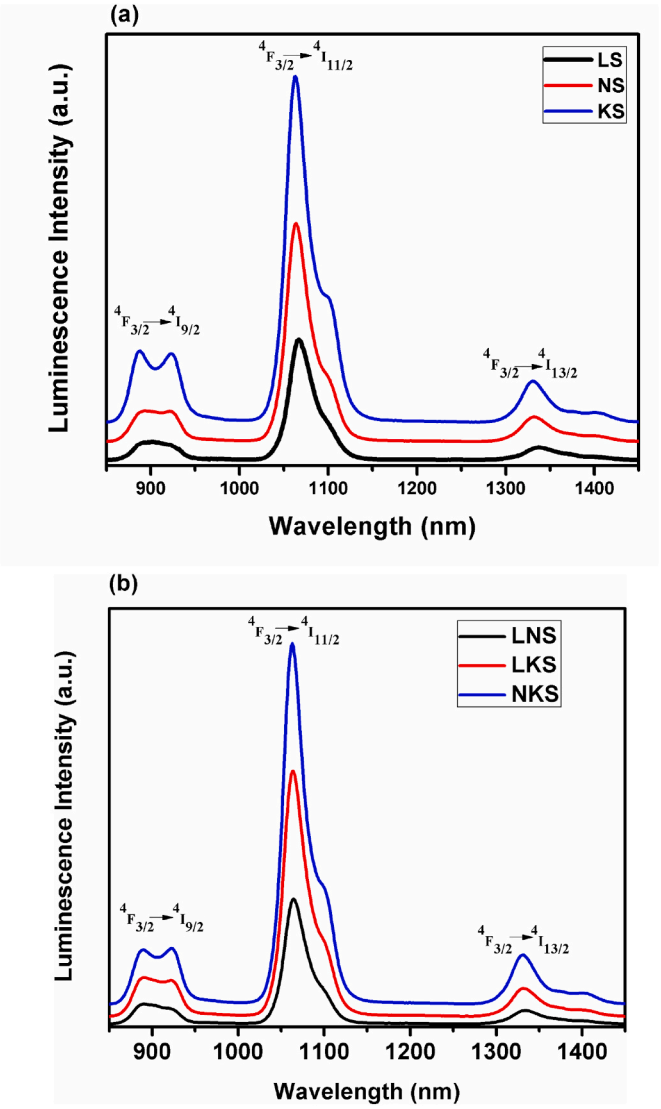

Fig. 5. NIR luminescence spectra of the alkali (a) and mixed alkali (b) metal silicate glasses doped with Nd^{3+}.

Table 6
Radiative transition probabilities A_{rad} (s^{-1}), branching ratio βR and radiative lifetime τrad (ms) for Nd^{3+} doped alkali and mixed alkali silicate glasses.

Transition from 4F3/2 to		ΔE (cm-1)			
			A_{rad} (s^{-1})	βR	τrad (ms)
LS-Nd	4I9/2	11064	130.85	0.318	2.434
	4I11/2	9372	236.25	0.575	
	4I13/2	7491	43.65	0.106	
NS-Nd	4I9/2	11248	154.13	0.372	2.414
	4I11/2	9407	220.44	0.532	
	4I13/2	7518	39.59	0.095	
KS-Nd	4I9/2	11273	105.25	0.433	4.120
	4I11/2	9497	117.30	0.483	
	4I13/2	7605	20.154	0.083	
LNS-Nd	4I9/2	11243	149.79	0.339	2.268
	4I11/2	9392	245.9	0.557	
	4I13/2	7504	45.07	0.102	
NKS-Nd	4I9/2	11274	229.05	0.470	2.053
	4I11/2	9414	221.12	0.454	
	4I13/2	7518	36.79	0.075	
LKS-Nd	4I9/2	11243	131.18	0.387	2.958
	4I11/2	9401	175.66	0.512	
	4I13/2	7511	31.211	0.091	

Table 7
Stimulated emission cross-section $\sigma(\lambda_p)$ for emission peak wavelengths λ_p in the infrared with effective line width values $\Delta\lambda_{eff}$ for Nd^{3+} doped alkali and mixed alkali silicate glasses.

Transition from 4F3/2 to				
		λ_p (nm)	$\Delta\lambda_{eff}$ (nm)	$\sigma(\lambda_p)$ x10^{-21} (cm^2)
LS-Nd	4I9/2	901	55.47	0.79
	4I11/2	1067	39.27	3.98
	4I13/2	1337	58.64	1.22
NS-Nd	4I9/2	921	59.47	0.98
	4I11/2	1063	39.44	3,76
	4I13/2	1332	54.97	1,20
KS-Nd	4I9/2	923	57.21	0.85
	4I11/2	1062	41.58	2.28
	4I13/2	1330	53.10	0.75
LNS-Nd	4I9/2	924	54.49	1.20
	4I11/2	1064	38.34	4.93
	4I13/2	1333	55.87	1.53
NKS-Nd	4I9/2	923	57.95	1.86
	4I11/2	1062	39.55	4.60
	4I13/2	1331	50.49	1.48
KLS-Nd	4I9/2	923	58.26	0.98
	4I11/2	1063	39.99	3.39
	4I13/2	1331	55.19	1.07

of the KS sample is relatively high compared to the other samples. The branching ratios are larger for 4F3/2 to 4I11/2 and decreases from Li, Na to K silicates.

Table 7 presents the results obtained for the stimulated emission cross-section $\sigma(\lambda_p)$, where λ_p is the emission peak wavelength and $\Delta\lambda_{eff}$ is the effective line width. The values for the combination of alkali ions are slightly larger. These results are like values reported in the literature for Nd^{3+} doped glasses [42–44].

4. Conclusions

FTIR and Raman spectra indicated some subtle changes in the silica network dependent on the alkali ion or mixture of them. The intensity of the emission bands in the NIR region of the samples containing K is relatively high compared to the samples containing Li and Na. The larger the volume of the alkali ion, the lower the values of the field strength, refractive index and density. The splitting induced by the Stark effect on the hypersensitive transition of Nd^{3+}, $^4I_{9/2} \rightarrow {}^4G_{5/2}$, $^2G_{7/2}$ is clearly seen, been more pronounced for the samples containing K. The spectroscopic quality factor is larger than 1 for sodium, potassium, sodium-potassium and lithium-potassium silicate glasses. The branching ratio is larger for 4F3/2 to 4I11/2 transition and decreases from Li, Na to K silicates. The stimulated emission cross-section obtained was similar to the values reported in the literature for Nd3+ in different glasses.

Funding

This work was supported by Brazilian agencies CAPES, CNPq and FAPERGS.

CRediT authorship contribution statement

Israel Montoya Matos: Conceptualization, Methodology, Resources, Writing - original draft, Writing - review & editing. **Naira M. Balzaretti:** Conceptualization, Methodology, Resources, Supervision, Validation.

Declaration of competing interest

The authors declare that they have no known competing financial interests or personal relationships that could have appeared to influence the work reported in this paper.

Data availability

The authors do not have permission to share data.

Acknowledgement

none.

References

[1] A.D. Pearson, S.P.S. Porto, W.R. Northover, Laser oscillations at 0.918, 1.057, and 1.401 microns in Nd^{3+}-doped borate glasses, J. Appl. Phys. 35 (1964) 1704–1706, https://doi.org/10.1063/1.1713723.
[2] M. Ganguli, M. Harish Bhat, K.J. Rao, Lithium ion transport in Li_2SO_4-Li_2O-P_2O_5 glasses, Solid State Ionics 122 (1999) 23–33, https://doi.org/10.1016/S0167-2738(99)00059-4.
[3] M. Dejneka, B. Samson, Rare-earth-doped fibers for telecommunications applications, Mater. Res. Soc. Bull. 24 (1999) 39–45, https://doi.org/10.1557/S0883769400053057.
[4] M.J. Weber, Glass for neodymium fusion lasers, J. Non-Cryst. Solids 42 (1980) 189–196, https://doi.org/10.1016/0022-3093(80)90021-6.
[5] B. Dunn, J. Zink, Optical properties of sol-gel glasses doped with organic molecules, J. Mater. Chem. 1 (1991) 903–913, https://doi.org/10.1039/JM9910100903.
[6] K. Gatterer, G. Pucker, W. Jantscher, H.P. Fritzer, A. Arafa, Suitability of Nd (III) absorption spectroscopic to probe the structure of glasses from the ternary system Na_2O-B_2O_3-SiO_2, J. Non-Cryst. Solids 231 (1998) 189–199, https://doi.org/10.1016/S0022-3093(98)00375-5.
[7] K. Gatterer, G. Pucker, H.P. Fritzer, S. Arafa, Hypersensitivity and nephelauxetic effect of Nd (III) in sodium borate glasses, J. Non-Cryst. Solids 176 (1994) 237–246, https://doi.org/10.1016/0022-3093(94)90082-5.
[8] Y.C. Ratnakaram, N.V. Shihari, A. Vijaya Kumar, D. Thirupathi Naidu, R.P. S. Chakradhar, Optical absorption and photoluminescence properties of Nd^{3+} doped mixed alkali phosphate glasses spectroscopic investigations, Spectroc. Acta Part A 72 (2009) 171–177, https://doi.org/10.1016/j.saa.2008.09.008.
[9] Y.C. Ratnakaram, A. Vijaya Kumar, D. Thirupathi Naidu, R.P.S. Chakradhar, K. P. Ramesh, Optical absorption and luminescence properties of Nd^{3+} in mixed alkali borate glasses—spectroscopic investigations, J. Luminesc. 110 (2004) 65–77, https://doi.org/10.1016/j.jlumin.2004.04.004.
[10] Y.C. Ratnakaram, S. Buddudu, Optical absorption spectra and laser analysis of Nd (III) in fluoroborate glasses, Solid St. Commun. 97 (1996) 651–655, https://doi.org/10.1016/0038-1098(95)00576-5.
[11] Y.C. Ratnakaram, N. Sudharani, Optical absorption spectra and Judd-Ofelt analysis of Nd^{3+} in certain chloroborate glasses, J. Phys. Chem. Solids 59 (1998) 215–219, https://doi.org/10.1016/S0022-3697(97)00162-5.
[12] Y.C. Ratnakaram, R.P.S. Chakradhar, K.P. Ramesh, J.L. Rao, J. Ramarkishna, The effect of host glass on optical absorption and fluorescence of Nd(3+) in xNa(2)O-(30-x)K(2)O-70B(2)O(3) glasses, J. Phys. Condens. Matter 15 (2003) 6715–6730, https://doi.org/10.1088/0953-8984/15/40/009.
[13] E. De La Rosa-Cruz, G.A. Kumar, L.A. Diaz-Torrs, A. Martinez, O. Barbosa-Garcia, Spectroscopic characterization of Nd^{3+} ions in barium fluoroborophosphate glasses, Opt. Mater. 18 (2001) 321–329, https://doi.org/10.1016/S0925-3467(01)00171-9.
[14] S. Duhan, S. Devi, M. Singh, Structural characterization of Nd-doped in silica host matrix prepared by wet chemical process, J. Rare Earths 27 (2009) 83–86, https://doi.org/10.1016/S1002-0721(08)60196-9.
[15] H. Namikawa, K. Arai, K. Kumuta, Y. Ishii, H. Tanaka, Preparation of Nd-doped SiO_2 glass by plasma torch CVD, Jpn. J. Appl. Phys. 2- Lett. 21 (1982) L360–L362, https://doi.org/10.1143/JJAP.21.L360.
[16] S. Sen, Atomic environment of high-field strength Nd and Al cations as dopants and major components in silicate glasses: a Nd L-III-edge and AlK-edge X-ray absorption spectroscopic study, J. Non-Crystal. Solids 261 (2000) 226–236, https://doi.org/10.1016/S0022-3093(99)00564-5.
[17] J.O. Isard, The mixed alkali effect in glass, J. Non-Crystal. Solids 1 (1969) 235–261, https://doi.org/10.1016/0022-3093(69)90003-9.
[18] D.E. Day, Mixed alkali glasses - their properties and uses, J. Non-Cryst. Solids 21 (1976) 343–372, https://doi.org/10.1016/0022-3093(76)90026-0.
[19] W.C. LaCourse, A defect model for the mixed alkali effect, J. Non-Crystal. Solids 95– 6 (1987) 905–912, https://doi.org/10.1016/S0022-3093(87)80697-X.
[20] F.C. Kracek, The ternary system K_2SiO_3-Na_2SiO_3-SiO_2, J. Phys. Chem. 36 (1932) 2529–2542, https://doi.org/10.1021/j150340a001.
[21] B.R. Judd, Optical absorption intensities of rare-earth ions, Phys. Rev. 127 (1962) 750–761, https://doi.org/10.1103/PhysRev.127.750.
[22] G.S. Ofelt, Intensities of crystal spectra of rare-earth ions, J. Chem. Phys. 37 (1962) 511–520, https://doi.org/10.1063/1.1701366.
[23] M.N. Muralidharan, C.A. Rasmitha, R. Rateesh, Photoluminescence and FTIR studies of pure and rare earth doped silica xerogels and aerogels, J. Porous Mater. 16 (2009) 635, https://doi.org/10.1007/s10934-008-9243-6.
[24] D.W. Matson, S.K. Sharma, J.A. Philpotts, The structure of high-silica alkali-silicate glasses – a Raman spectroscopy investigation, J. Non-Crystal. Solids 58 (1983) 323–352, https://doi.org/10.1016/0022-3093(83)90032-7.

[25] H. Doweidar, The density of alkali silicate glasses in relation to the microstructure, J. Non-Cryst. Solids 194 (1996) 155–162, https://doi.org/10.1016/0022-3093(95)00489-0.
[26] S. Giri, C. Gaebler, J. Helmus, M. Affagiato, S. Feller, M. Kodama, A general study of packing in oxide glass systems containin alkali, J. Non-Cryst. Solids 347 (2004) 87–92, https://doi.org/10.1016/j.jnoncrysol.2004.08.103.
[27] H. EbendorffHeidepriem, E. Ehrt, Spectroscopic properties of Eu^{3+} and Tb^{3+} ions for local structure investigations of fluoride phosphate and phosphate glasses, J. Non-Cryst. Solids 208 (1996) 205–216, https://doi.org/10.1016/S0022-3093(96)00524-8.
[28] W.T. Carnall, P.R. Fields, K. Rajnak, Spectral intensities of trivalent lanthanides and actinides in solution .1. Pr^{3+}, Nd^{3+}, Pm^{3+}, Sm^{3+}, Dy^{3+}, Ho^{3+}, Er^{3+} and Tm^{3+}, J. Chem. Phys. 49 (1968) 4424–4442, https://doi.org/10.1063/1.1669893.
[29] I.M. Montoya, N.M. Balzaretti, High pressure effect in the near-infrared emission of Nd3+-doped alkali silicate glasses, High Pres. Res. 42 (1) (2022) 1–13, https://doi.org/10.1080/08957959.2021.2012570.
[30] I.R. Montoya Matos, A. Carrillo Herrera, S. Buchner, N.M. Balzaretti, Lanthanide-doped glasses under high pressure, in: En I.S. Butle (Ed.), High-pressure Molecular Spectroscopy, De Gruyter, 2022, pp. 227–237, https://doi.org/10.1515/9783110668612-007.
[31] M.V.S. Kumar, D. Rajesh, A. Balakrishna, Y.C. Ratnakaram, Thermal and optical properties of Nd^{3+} doped lead zinc borate glasses - influence of alkali metal ions, Physica B 415 (2013) 67–71, https://doi.org/10.1016/j.physb.2013.02.004.
[32] C.K. Jorgensen, R. Reisfeld, Judd-Ofelt parameters and chemical bonding, J. Less Comm. Metals 93 (1983) 107–112, https://doi.org/10.1016/0022-5088(83)90454-X.
[33] H. Takebe, K. Morinaga, T. Izumitani, Correlation between radiative transition-probabilities of rare-earth ions and composition in oxide glasses, J. Non-Cryst. Solids 178 (1994) 58–63, https://doi.org/10.1016/0022-3093(94)90265-8.
[34] J. Stone, C.A. Burrus, Neodymium-doped silica lasers in end-pumped fiber geometry, Appl. Phys. Lett. 23 (1973) 388–389, https://doi.org/10.1063/1.1654929.
[35] G.N.H. Kumar, J.L. Rao, K.R. Prasad, Y.C. Ratnakaram, Fluorescence and Judd-Ofelt analysis of Nd^{3+} doped P_2O_5-Na_2O-K_2O glass, J. Alloys Comp. 480 (2009) 208–215, https://doi.org/10.1016/j.jallcom.2009.02.033.
[36] R.R. Jacobs, M.J. Weber, Dependence of 4F3-2 -] 4K11-2 induced-emission cross-section for Nd^{3+} on glass composition, IEEE J. Quantum Electron 12 (1976) 102–111, https://doi.org/10.1109/JQE.1976.1069101.
[37] P. Nachimuthu, M. Vithal, R. Jagannathan, Absorption and emission spectral properties of Pr^{3+}, Nd^{3+}, and Eu^{3+} ions in Heavy-metal oxide glasses, J. Am. Cem. Soc. 2004 83 (3) (2004) 597–604, https://doi.org/10.1111/J.1151-2916.2000.TB01238.X.
[38] I.M. Montoya, N.M. Balzaretti, High pressure effect on structural and spectroscopic properties of Sm3+-doped alkali silicate glasses, High Pres. Res. 37 (3) (2017) 296–311.
[39] I.R.M. Matos, Influence of alkali metal ions on the structural and spectroscopic properties of Sm^{3+}-doped silicate glasses, Ceramics 6 (2023) 1788–1798, https://doi.org/10.3390/ceramics6030109.
[40] Y. Nageno, H. Takebe, K. Morinaga, Correlation between radiative transition-probabilites of Nd^{3+} and composition in silicate, borate and phosphate- glasses, J. Am. Ceram. Soc. 76 (1993) 3081–3086, https://doi.org/10.1111/j.1151-2916.1993.tb06612.x.
[41] M. Ajroud, M. Haouari, H. Ben Ouada, H. Maaref, A. Brenier, C. Garapon, Investigations of the spectroscopic properties of Nd^{3+}- doped phosphate glasses, J. Phys. Condens. Matter 12 (2000) 3181–3193, https://doi.org/10.1088/0953-8984/12/13/324.
[42] G.N.H. Kumar, J.L. Rao, K.R. Prasad, Y.C. Ratnakaram, Fluorescence and Judd-Ofelt analysis of Nd^{3+} doped P_2O_5-Na_2O-K_2O glass, J. Alloys Comp. 480 (2009) 208–215, https://doi.org/10.1016/j.jallcom.2009.02.033.
[43] K. Upendra Kumar, P. Babu, K. Hyuk Jang, H. Jin Seo, C.K. Jayasankar, A.S. Joshi, J. Spectroscopic and 1.06 μm laser properties of Nd^{3+} doped K-Sr-Al phosphate and fluorophosphate glasses, Alloys Comp 458 (2008) 509–516, https://doi.org/10.1016/j.jallcom.2007.04.035.
[44] K. Upendra Kumar, V.A. Prathyusha, P. Babu, C.K. Jayasankar, A.S. Joshi, A. Speghini, M. Bettinelli, Fluorescence properties of Nd^{3+} doped tellurite glasses, Spectrochim. Acta, Part A 67 (2007) 702–708, https://doi.org/10.1016/j.saa.2006.08.027.